ISSN 1330-3651 (Print), ISSN 1848-6339 (Online) https://doi.org/10.17559/TV-20250705002798
Original scientific paper

Effect of Crosswind on Drag and Lift Variations during Mixed-Vehicle Overtaking Manoeuvres: A CFD Approach

Daniela Delia ALIC*, Luisa Izabel DUNGAN, Milan RACKOV, Marian GRECONICI, Carmen Inge ALIC

Abstract: A CFD-based analysis is carried out in this study to examine time-dependent aerodynamic effects during highway overtaking manoeuvres, with a primary focus on truck-truck interactions under crosswind conditions. Using ANSYS Fluent and unsteady Reynolds-Averaged Navier-Stokes (RANS) simulations, the time-resolved aerodynamic behaviour of a truck being overtaken by an identical vehicle is investigated in detail. A secondary case involving a passenger car overtaking the truck is also examined for comparative purposes. The analysis concentrates on the evolution of the drag and lift coefficients of the overtaken truck throughout the overtaking process. Results indicate that truck-truck interactions produce stronger aerodynamic disturbances, with greater fluctuations in drag and lift compared to the car-truck scenario. These effects are strongly dependent on vehicle spacing and relative positioning. The findings highlight the critical role of transient aerodynamic loading in the design and operation of heavy-duty vehicles, particularly in mixed traffic environments and crosswind-prone areas. This research advances the understanding of real-world aerodynamic interactions, with implications for fuel efficiency, dynamic stability, and highway safety.

Keywords: aerodynamic stability; CFD; crosswind effects; overtaking manoeuvres; transient aerodynamics; truck-truck interaction; wake dynamics

1 INTRODUCTION

Aerodynamic forces are central in the design, performance, and safety of road vehicles, particularly in situations with dense, high-velocity vehicle flow, as highways. Among these forces, aerodynamic drag significantly influences fuel consumption and overall efficiency, while lift and lateral forces directly affect vehicle handling and stability [1]. Understanding how these forces vary during transient interactions, such as overtaking manoeuvres, is important for improving the performance of vehicle and ensuring road safety - especially for heavy-duty trucks, which are susceptible to aerodynamic disturbances [2].

Crosswinds disrupt the symmetry of airflow around the vehicle body [3], creating unbalanced pressure distributions [4] and altering the behaviour of aerodynamic forces [5]. In scenarios involving multiple vehicles, such as truck-truck or truck-car overtaking [6], the influence of lateral wind can lead to substantial variations in drag and lift coefficients [7]. These variations can compromise vehicle stability and increase energy losses [8], making crosswind effects an important consideration in both vehicle design and traffic safety analysis [9, 10].

The latest developments in intelligent driver support systems and autonomous driving solutions have increased the relevance of detailed aerodynamic modelling. Vehicles using such systems operate in close-proximity configurations, including platooning [11], where small aerodynamic disturbances may lead to large control corrections or reduced energy efficiency under crosswind conditions [12].

This study employs computational fluid dynamics (CFD) to analyse unsteady aerodynamic behaviour of vehicles during overtaking manoeuvres under varying crosswind intensities. Using Reynolds-Averaged Navier-Stokes (RANS) simulations in ANSYS Fluent [13], the research focuses primarily on truck-truck interactions, with truck-car results from previous work [14] included for comparison. The study analyses the evolution of drag and lift coefficients, velocity and pressure fields, and Reynolds number distributions across four overtaking phases.

The results provide insight into the aerodynamic shielding effect, flow separation patterns, and transient force behaviour in realistic traffic scenarios. These findings aid to the development of stable and fuel-efficient heavy-duty vehicles and support the optimization of traffic management strategies in crosswind-prone environments [15].

2 THEORETICAL AND NUMERICAL SETUP

The theoretical foundation for airflow CFD modelling are the Navier-Stokes equations, which describe the motion of viscous fluids, through a system of coupled nonlinear partial differential equations. The unknowns, three velocity components and two thermodynamic variables (pressure and density or energy) are linked through an equation of state. They enforce the conservation laws governing mass (via the continuity equation), momentum (based on Newton's second law), and energy (in accordance with the first law of thermodynamics) [16].

In this work, the turbulent flow is modelled using a two-equation eddy-viscosity formulation, namely the Shear Stress Transport (SST) k-ω model, which approximates the Reynolds-Averaged Navier-Stokes (RANS) equations and is known for its accuracy in predicting boundary layer behaviour and flow separation, in strong correlation with experimental results. The RANS approach solves for the time-averaged flow field while accounting for the influence of turbulence through modelled fluctuations [13].

State-of-the-art CFD tools such as ANSYS Fluent are widely used in the automotive sector for analysing the aerodynamic behaviour of vehicles, due to their robust physics modelling capabilities and high accuracy, proving their contribution even in terms of the aerodynamic characteristics of race cars [17]. With increasing traffic and the development of safety-enhancing technologies, CFD simulations are commonly employed to evaluate drag and lift coefficients, optimize vehicle spacing, and assess stability in various driving conditions and mixed scenarios [18]. Overtaking manoeuvres lead to airflow interactions between vehicles, resulting in transient aerodynamic

effects that can affect vehicle control. These effects are particularly significant in the presence of crosswind, leading to sudden changes in pressure and flow velocity that may compromise handling.

This study, carried out using an efficient numerical model in ANSYS Fluent to evaluate crosswind effects on vehicle aerodynamics, offers meaningful insights into the qualitative aerodynamic behaviour of heavy-duty vehicles like European-style trucks (10,5 × 2,5 × 4 m) [19] in conditions of highway traffic. The simulated scenarios focus on overtaking manoeuvres at a vehicle speed of approximately 28 m/s, subjected to lateral wind speeds categorized as weak (5 m/s), moderate (10 m/s), and strong (15 m/s). For comparison, results from a previous aerodynamic study [5] involving a passenger car (BMW 1 Series, 4,3 × 1,8 × 1,43 m) [20] overtaking a European-style truck are employed. Air is modelled with standard properties (density 1,225 kg/m³, viscosity $1{,}7894 \times 10^{-5}$ kg/m × s), and inlet turbulence conditions are set at 1% intensity and a viscosity ratio of 2.

The overtaking process is analysed in four traffic phases: the truck on the second lane is positioned behind (Fig. 1), alongside (Fig. 2) and ahead (Fig. 3) of the truck on the first lane, then moves on the first lane in front of the overtaken truck, marking the beginning of a platoon configuration (Fig. 4). These scenarios are used to assess the disturbances experienced by both vehicles, offering a qualitative understanding of the aerodynamic patterns of crosswinds, and to quantify their effect on vehicle stability, in terms of lift and drag.

The numerical simulations are performed in a rectangular volume computational domain, measuring 24 m in height, 40 m in width, and 50 m in length. Boundary conditions are set as: velocity inlets - the front (*yz*) and right (*yx*) boundaries, corresponding to the incoming airflow in the longitudinal (+*x*), respectively lateral (+*z*) directions; pressure outlets - the rear (*yz*) and left (*yx*) boundaries, in order to allow free outflow; stationary shear-free wall - the top surface (*xz*); moving no-slip wall - the ground (*xz*) surface, for simulating road-relative vehicle motion. Both the car and truck surfaces are defined as stationary no-slip walls. The no-slip boundary condition, assuming zero relative velocity between the fluid and the wall, is applied to all solid surfaces in contact with the fluid. This condition reflects the physical behaviour of viscous flows, where adhesive forces between fluid and solid particles dominate over cohesive forces within the fluid, resulting in zero fluid velocity at the wall interface.

Discretization of the governing equations is performed through the Finite Volume Method, employing the Least Squares Cell-Based approach for evaluating spatial derivatives [21]. Pressure-velocity coupling is handled using a Coupled Scheme that incorporates the Rhie-Chow interpolation method [22], to avert pressure-velocity decoupling and ensure robust momentum flux computation. This approach offers improved stability and convergence behaviour compared to traditional segregated algorithms, particularly in steady-state single-phase flow simulations.

To enhance the accuracy of turbulent flow prediction around the vehicle surfaces, second-order upwind discretization schemes are employed for both the Turbulent Kinetic Energy (k) and Specific Dissipation Rate (ω) equations [16]. Additionally, the External-Aero Favourable Settings are enabled during Hybrid Initialization to produce a realistic initial velocity field suited for external flow simulations.

The fluid domain was discretized using poly-hexcore elements, with cell sizes ranging from 0.0488 m to 1.5625 m, following the ANSYS Fluent Meshing Watertight Geometry procedure. Two localized mesh refinement zones were introduced around the vehicles, employing adaptive surface meshing with a growth rate of 1.1999. The refinement settings included automatic detection of minimum and maximum cell sizes, a curvature normal angle threshold of 18°, and three fluid-wall boundary layers with smooth transitions, defined by a transition ratio of 0.272 and a growth rate of 1.2. As a result, the mesh quality indicators show, depending on the case/setup, an average skewness of 0.023-0.024, considered excellent for values below 0.25, and an average orthogonal quality of 0.86-0.97, which is classified as very good (with 1 being ideal). Refined meshing in key flow regions ensures sufficient resolution to accurately capture velocity gradients and flow separation phenomena.

In ANSYS Fluent steady-state simulations, the Time Scale Factor is part of the pseudo-transient approach, which enhances convergence by simulating transient-like behavior without fully resolving the time-dependent equations. Setting the Time Scale Factor to 1 instructs Fluent to apply a pseudo time step equal to the default time scale computed automatically for each control volume. While steady-state simulations do not account for actual time progression, this method helps improve stability and convergence, particularly in challenging cases such as high-speed flows or turbulence, and can prevent divergence caused by large initial imbalances in the residuals. Convergence is assessed by monitoring the residuals of the continuity and momentum equations, along with the turbulence variables k and ω. The solution is considered converged when all residuals fall below 10^{-4}, indicating that the simulation has reached a numerically stable and accurate state.

3 ANALYSIS AND RESULTS

3.1 Comparative Analysis of Aerodynamic Interactions

An in-depth investigation of the overtaking process - featuring vehicles traveling in close proximity across four different relative configurations - uncovers significant aerodynamic interactions. These interactions impact vehicle behaviour and stability, as reflected by variations in flow velocity and pressure fields, changes in drag coefficients, and differences in Reynolds numbers. The study systematically examines these aerodynamic effects, emphasizing their relevance to safety and energy efficiency in crosswind-prone environments.

The plots in Fig. 1 to Fig. 4 illustrate four distinct overtaking phases, presented in top view (*xz* plane, corresponding to the road surface). Each phase visualizes the velocity field pattern and corresponding vector magnitudes, pathlines of the induced flow, and corresponding turbulent Reynolds number distribution.

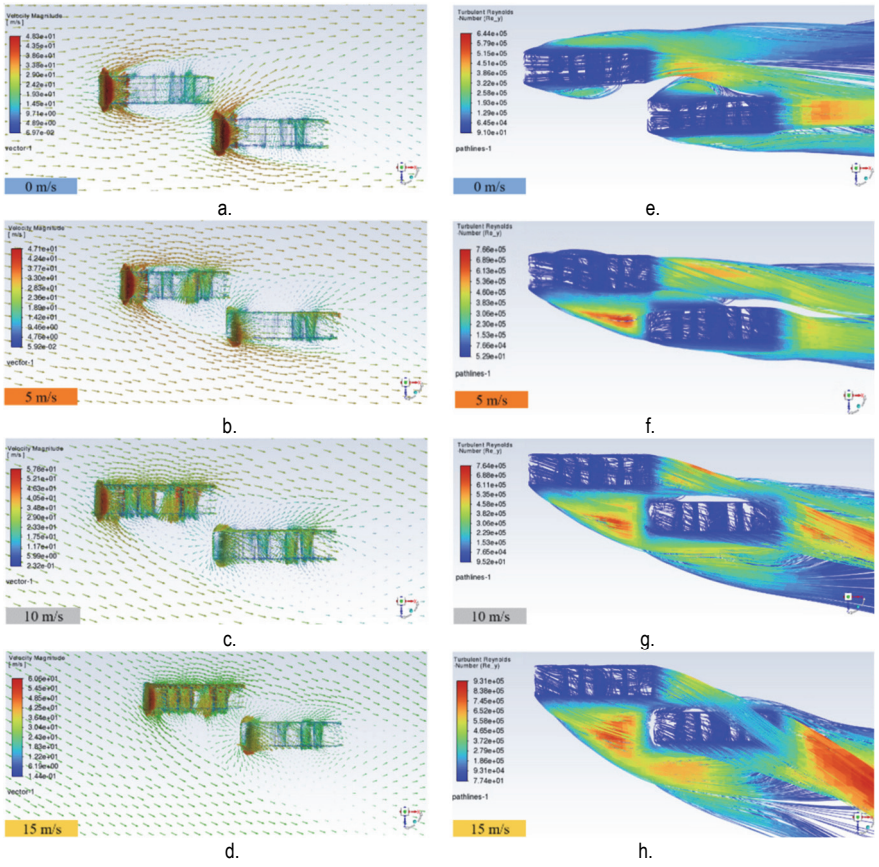

Figure 1 Overtaking phase 1. Airflow velocity field pattern and corresponding vector magnitudes, pathlines of the induced flow and turbulent Reynolds number distribution

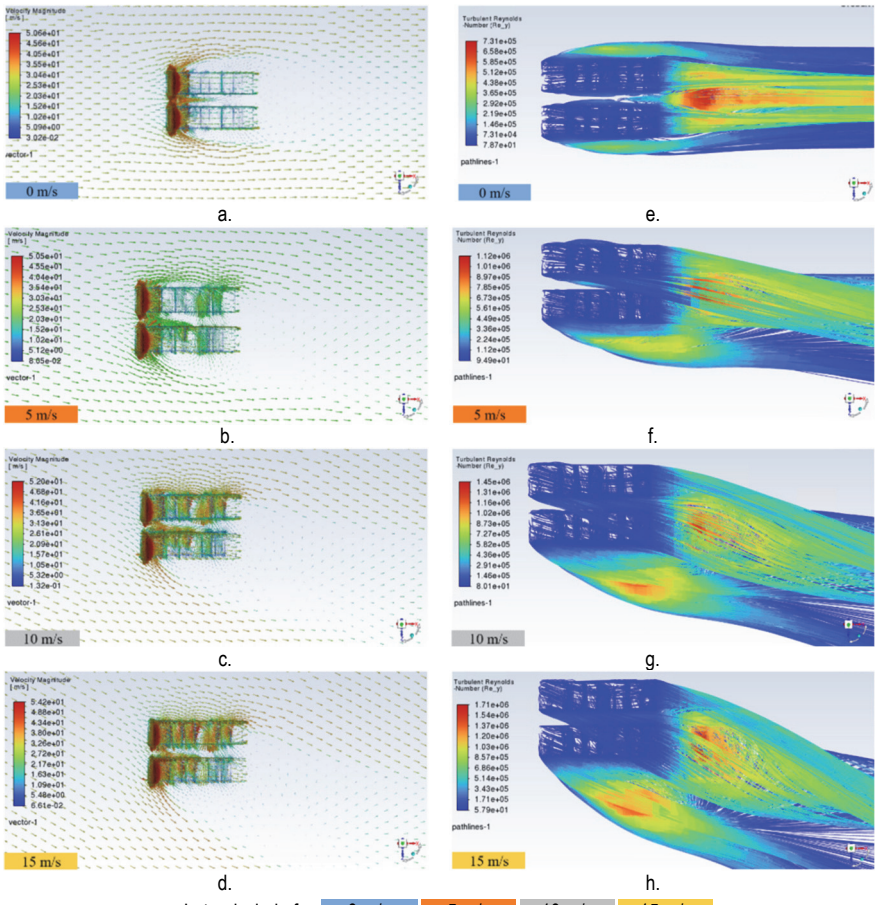

Figure 2 Overtaking phase 2. Airflow velocity field pattern and corresponding vector magnitudes, pathlines of the induced flow and turbulent Reynolds number distribution

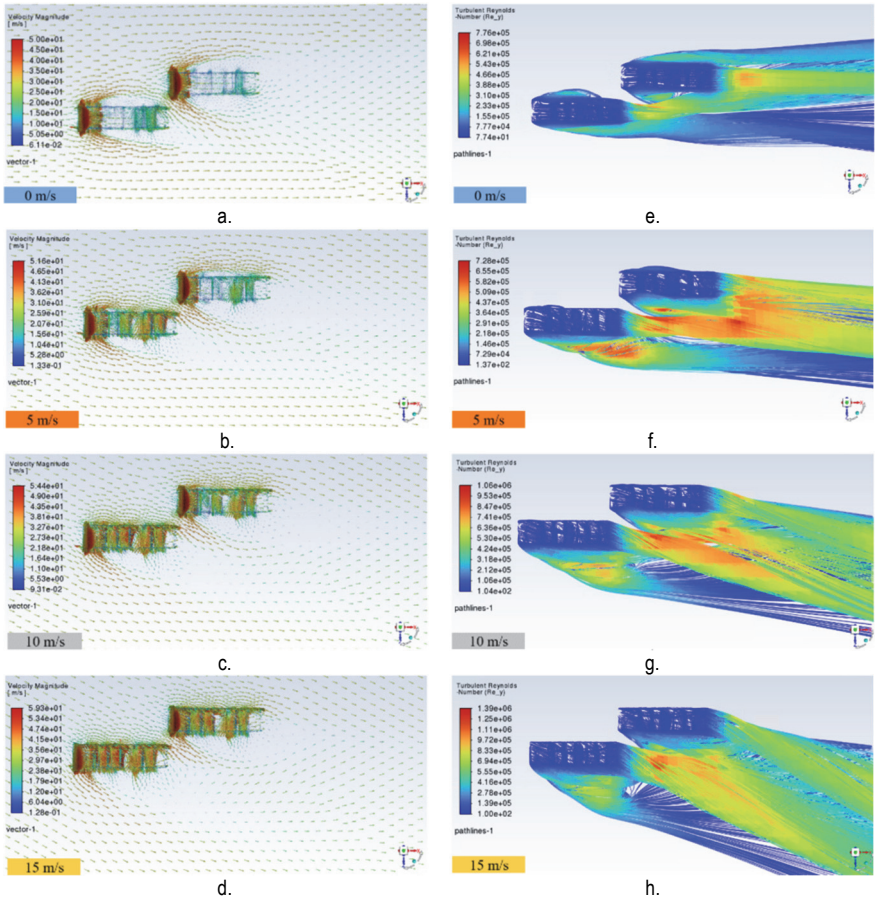

Figure 3 Overtaking phase 3. Airflow velocity field pattern and corresponding vector magnitudes, pathlines of the induced flow and turbulent Reynolds number distribution

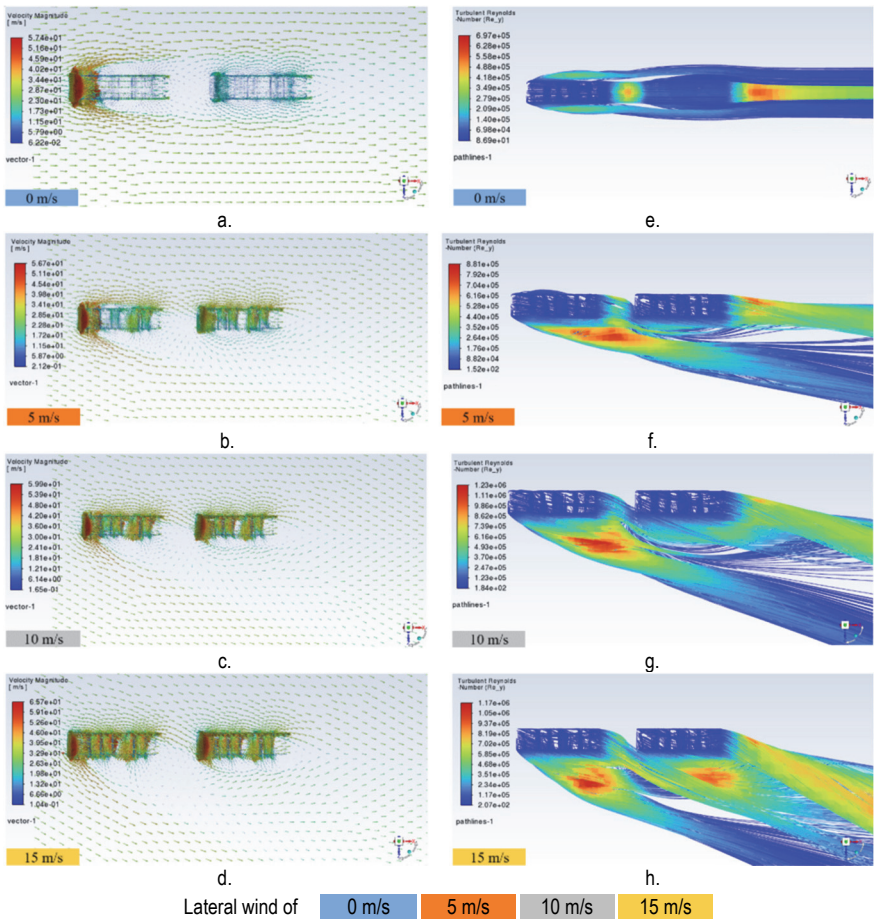

Figure 4 Overtaking phase 4. Airflow velocity field pattern and corresponding vector magnitudes, pathlines of the induced flow and turbulent Reynolds number distribution

The analysis begins with a case of zero lateral wind - representing only head-on airflow due to vehicle motion - and progresses to crosswind conditions of up to 15 m/s. When lateral wind is not present, the aerodynamic flow around both vehicles behaves as predicted, with only minor distortions in the (x) direction (of travel) caused by the aerodynamic interaction between the vehicles travelling in adjacent lanes, Fig. 1a. The Reynolds number plots in this case indicate predominantly laminar flow over the vehicle surfaces (maximum values around 10^5), transitioning to mildly turbulent flow in the wake regions Fig. 1e. As a side note, the plots display local Reynolds numbers calculated by ANSYS Fluent using local velocity and characteristic length scales. Thus, the pathlines represent flow behaviour relative to nearby surfaces or localized regions. Additionally, the visualized areas are close to the truck walls, where boundary layer effects reduce airflow velocity.

As crosswind intensity increases, the overall flow field undergoes significant changes. The lead vehicle in the windward lane acts as a lateral aerodynamic shield for the following vehicle, generating a region of reduced airflow velocity on the leeward side, Fig. 1b to Fig. 1d. This shielding effect alters the pressure distribution and flow behaviour around the second vehicle. Under strong crosswind conditions (15 m/s), the Reynolds numbers increase significantly, reaching values close to 10^6, indicating a transition toward turbulent flow, Fig. 1h. This transition is not limited to the wake region but extends along the lateral surfaces of the downstream vehicle, particularly on the side exposed to the diverted cross flow.

In the second phase of the analysis, Fig. 2, the vehicles are moving side by side. Comparing the zero crosswind cases in phases 1 (Fig. 1a) and 2 (Fig. 2a), an increase in the maximum airflow velocity in the longitudinal (x) direction is observed. Velocity contour plots show a complete stagnation of airflow at the front of each vehicle, followed by acceleration over their surfaces. This behaviour creates a high-pressure zone at the vehicle front, more pronounced for the trucks than for the car [14], due to their larger frontal area and blunter geometry.

Under crosswind conditions, the high-pressure area extends toward the windward side of the truck occupying the upwind lane (Fig. 2b to Fig. 2d). The primary stagnation points are located at the front and on the side facing the wind, where the airflow slows down before diverting and accelerating along the truck's surface. At the rear, the flow detaches from the vehicle, generating a wake characterized by recirculating flow. Owing to the truck's sharp geometric transitions and the high Reynolds number regime, flow separation occurs more abruptly and over a larger area than it does for the car [14], leading to considerably larger wake zones and increased aerodynamic drag (Fig. 5 and Fig. 6).

With the intensification of crosswinds, the truck in the windward lane disturbs both the frontal and lateral airflow patterns, redirecting the incoming streamlines nearly tangentially across the windward side of the leeward vehicle (Fig. 2d).

The Reynolds number distribution in this phase exhibits similar characteristics to those observed in phase 1, with peak values approaching 10^6, in the wake regions and along the wind-protected lateral surfaces (Fig. 2f to Fig. 2h), where separated airflow tends to reattach.

For the third phase of the study, the vehicle in the second lane becomes entirely impacted by the oncoming air stream and the crosswind (Fig. 3). Despite this full exposure, the aerodynamic influence of the truck in the first lane remains evident, particularly through the disturbed velocity field (Fig. 3a to Fig. 3d) and wake structures observed in its proximity.

The flow field continues to exhibit Reynolds number peaks on the order of 10^6, around regions of separated flow, especially near the rear and lateral surfaces of the truck (Fig. 3e to Fig. 3h). These values indicate a transitional regime, where the flow is developing into turbulence. Effective modelling of turbulence plays a key role in predicting external vehicle flow behaviour, especially since increased Reynolds numbers tend to amplify turbulence and resistance [23, 24]. The present study prioritizes computational efficiency, the simulations are performed using available computational resources and are intended to provide a reliable estimation of crosswind effects on aerodynamic performance, rather than fully resolved turbulence predictions.

Flow separation along the frontal and side surfaces of the vehicles leads to the formation of high-pressure, low-speed regions that significantly increase pressure drag.

In calm conditions, the airflow remains relatively streamlined, supporting lower drag coefficients. However, under crosswind conditions, the flow becomes highly disturbed and less organized around both vehicles. This disruption leads to increased aerodynamic resistance and a corresponding rise in drag coefficients, which, in some cases, exceed a value of one [25].

3.2 Comparative Analysis of the Drag Coefficients

In the first phase of the analysis (Fig. 5 and Fig. 6 - Phase 1), increasing the lateral wind velocity results in a reduction of drag in the longitudinal (x) direction for both vehicles travelling on the second lane. This reduction facilitates their forward motion, as the truck in the windward lane acts as an aerodynamic shield, diminishing their direct exposure to the crosswind. In the lateral (z) direction, the car experiences minimal aerodynamic force, with values directed toward the truck - indicated by negative drag components - suggesting a slight lateral push of the car toward the adjacent truck [14]. Simultaneously, the airflow velocity over the truck in the first lane increases with crosswind intensity, reaching peak drag coefficient values exceeding 1, not only at the front windshield but also along the windward side and upper surfaces of the truck body. This accelerated flow contributes to increased aerodynamic drag in the x and z directions, indicating that the truck in the first lane is subjected to a combined force pushing it both rearward and laterally toward the vehicle in the second lane.

At the next phase of the study (Fig. 5 and Fig. 6 - Phase 2), as the lateral wind intensity increases, the car experiences a decreased drag in the longitudinal (x) direction. The observed reduction results from the aerodynamic sheltering caused by the truck in the first lane, which alters both the front and side airflow, channelling it nearly tangentially along the car's body [14]. This partial

shielding lowers the pressure differential acting on the car, thereby reducing its drag. Conversely, in the lateral (z) direction, the aerodynamic force on the car increases, pushing it away from the adjacent truck due to the redirected crosswind flow.

The aerodynamic behaviour of the truck in the second lane differs notably. Owing to its consistent positioning in the lee of the truck in the first lane, it remains continuously shielded from the full impact of the crosswind.

As a result, both its longitudinal and lateral drag components remain relatively constant throughout this phase.

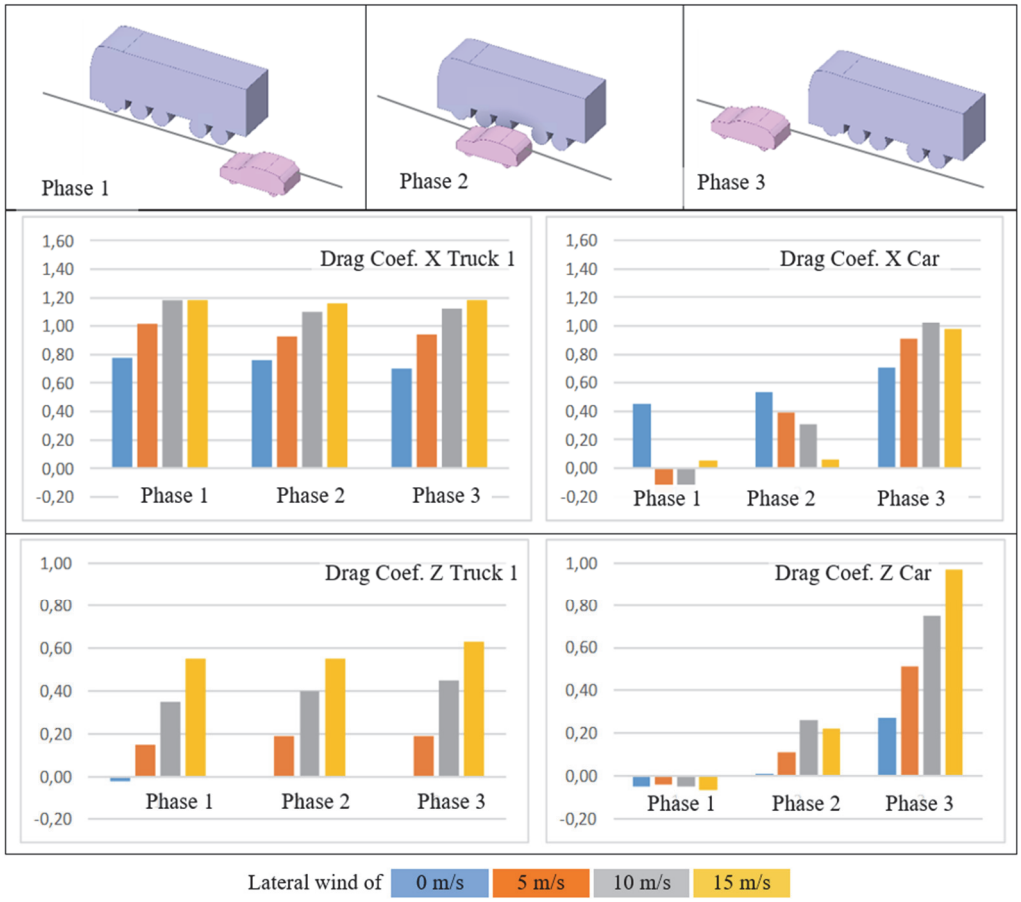

Figure 5 Truck-car overtaking manoeuvres - comparative changes in drag coefficients along *x* and *z* directions at lateral wind of 0 m/s, 5 m/s, 10 m/s, 15 m/s

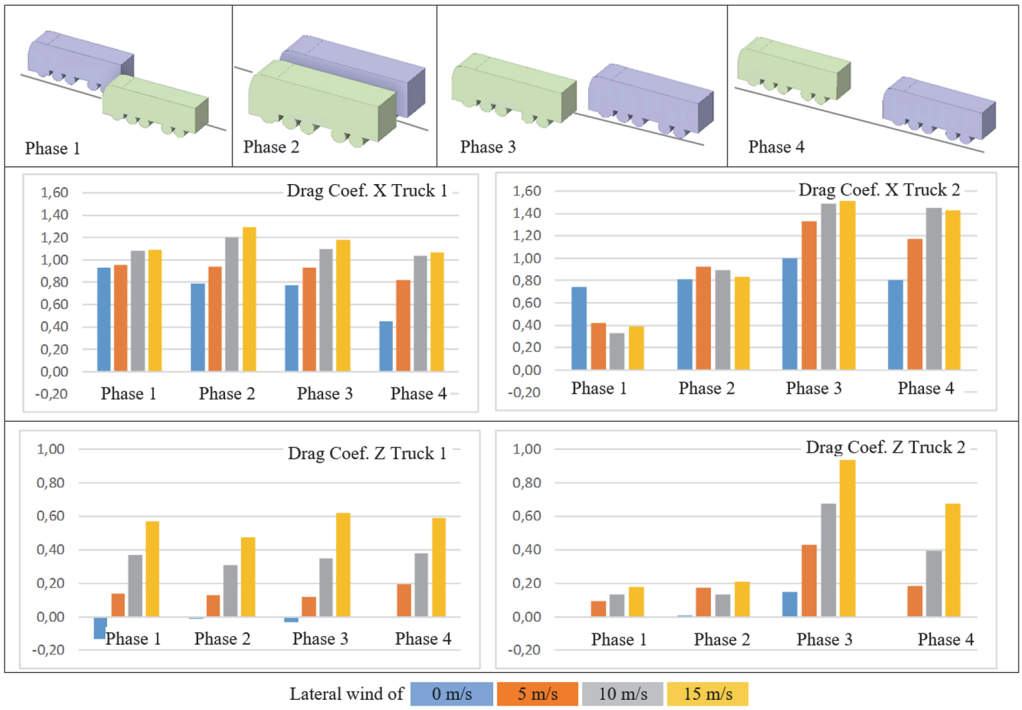

Figure 6 Truck-truck overtaking manoeuvres - comparative changes in drag coefficients along *x* and *z* directions at lateral wind of 0 m/s, 5 m/s, 10 m/s, 15 m/s

During the third phase (Fig. 5 and Fig. 6 - Phase 3), aerodynamic drag increases substantially in both the longitudinal (x) and lateral (z) directions, as a result of stronger crosswind conditions and the complete exposure of the vehicle in the second lane. This increased exposure results in greater pressure differentials across the vehicle surfaces, leading to elevated drag coefficients. In contrast, the drag coefficients of the truck in the first lane remain comparable to those computed in phase 2, as its aerodynamic behaviour is not substantially affected by the position or motion of the vehicle in the adjacent lane.

A fourth phase under investigation (Fig. 5 and Fig. 6 - Phase 4) focuses on the truck-truck interaction immediately after overtake at the beginning of platooning, where the trailing truck follows at a distance of approximately half a vehicle length (around 5 meters). In this configuration, the leading truck (Truck 2) provides aerodynamic shielding for the following vehicle (Truck 1). This effect is particularly pronounced under calm wind conditions, where a significant reduction in the drag coefficient is observed - up to 50% compared to the isolated case. However, as crosswind intensity increases, the aerodynamic benefit of platooning diminishes. Under strong lateral wind conditions, the drag reduction remains limited to the direction of travel and decreases in effectiveness, with observed differences in the drag coefficient reduced to approximately 20-30%.

3.3 Comparative Analysis of the Lift Coefficients

When a vehicle is subjected to crosswind conditions, the airflow around it becomes asymmetric, disrupting the typical front-to-rear streamlines. This effect induces pressure imbalances along the vehicle's surfaces, causing variability in the generated lift force. While the lift coefficients are generally low (typically < 0,1), specific flow interactions can lead to notable aerodynamic effects, as summarized below:

- Lane shielding effect: The lead vehicle travelling in the windward lane provides aerodynamic shielding for the vehicle in the adjacent (leeward) lane. This reduces the crosswind exposure of the latter, significantly decreasing its lift and in some cases generating a localized downforce.
- Crosswind exposure during overtaking: Initially, the crosswind induces a lift increase due to the pressure imbalance between the windward and shielded sides of the overtaken vehicle. As the relative positions change during the overtaking manoeuvre, the shielding effect is re-established, reducing the lift. In truck-truck interactions, however, the lift coefficient of the overtaken truck continues to rise slightly due to sustained airflow interference.
- Full exposure of passenger cars: As the car becomes completely exposed to lateral wind, a pressure differential across its sides generates a noticeable initial lift [14]. This is followed by a reduction in lift as the flow stabilizes and pressure on the windward side balances out. Overall, lift coefficients remain below 0,2.
- Rear truck lift under strong crosswind: The trailing truck, particularly in strong crosswind conditions (15 m/s), can develop lift coefficients as high as 0,25. While this value is insufficient to cause physical lift-off, it may reduce tire grip and increase susceptibility to rollover or lateral instability, especially in the presence of gusts or abrupt steering inputs.

4 CONCLUSION

Accurate prediction and reduction of aerodynamic drag are fundamental objectives in automotive engineering, directly contributing to increased vehicle performance, improved fuel efficiency, and enhanced operational safety [26].

Among the various environmental factors influencing aerodynamic behaviour, crosswinds play a particularly critical role [27], especially in scenarios involving fast-moving traffic on major roads with reduced inter-vehicle distances and overtaking manoeuvres [28]. Crosswinds can significantly modify the aerodynamic force distribution around vehicles, leading to pronounced and rapid fluctuations in drag coefficients [29]. These variations can have an unfavourable effect on vehicle handling and stability, as well as fuel consumption, thereby posing potential risks to road safety.

The expanding implementation of ADAS and the forthcoming integration of self-driving vehicles emphasize the necessity of reliable aerodynamic analysis under crosswind influences. Vehicles operating in convoys or platoons are particularly sensitive to crosswind-induced disturbances, which can compromise energy efficiency and introduce control challenges. Therefore, developing reliable numerical models to compute the aerodynamic interplay between vehicles under crosswind conditions is fundamental for refining vehicle performance and supporting next-generation transportation systems.

This research investigates the unsteady aerodynamic effects induced by crosswinds during interactions between different vehicle types (truck-truck versus truck-car) in highway traffic scenarios. Using advanced computational fluid dynamics (CFD) techniques, the study examines how drag forces evolve under various crosswind strengths and relative positioning setups, simulating realistic high-speed traffic conditions where vehicles operate in close proximity.

The findings improve knowledge of the aerodynamic mechanisms involved and offer actionable insights for optimizing vehicle geometry and traffic configurations to mitigate adverse aerodynamic effects. Additionally, the study supports the development of crosswind-resilient vehicle designs and informs strategies for adaptive speed limit recommendations under moderate to strong wind conditions, promoting safer and more energy-efficient highway transportation.

5 REFERENCES

[1] Ekman, P. (2020). *Important Factors for Accurate Scale-Resolving Simulations of Automotive Aerodynamics*. PhD Dissertation, Linköping University, Linköping Electronic Press. https://doi.org/10.3384/diss.diva-164926

[2] Askerdal, M., Fredriksson, J., & Laine, L. (2023). Development of simplified air drag models including crosswinds for commercial heavy vehicle combinations. *Vehicle System Dynamics*, *62*(5), 1085-1102. https://doi.org/10.1080/00423114.2023.2213786

[3] Levin, J. & Chen, S. H. (2022). Flow Structure Investigation of a Truck under Crosswinds. *Journal of Applied Fluid Mechanics*, *15*(5), 1513-1523. https://doi.org/10.47176/jafm.15.05.1076
[4] Minelli, G., Adi Hartono, E., Chernoray, V., Hjelm, L. & Krajnovic, S. (2017). Aerodynamic flow control for a generic truck cabin using synthetic jets. *Journal of Wind Engineering & Industrial Aerodynamics*, *168*, 81-90. https://doi.org/10.1016/j.jweia.2017.05.006
[5] Alic, D., Miltenović, A., Banić, M., & Vicente Zafra, R. (2025). Numerical Investigation of Large Vehicle Aerodynamics under the Influence of Crosswind. *Spectrum of Mechanical Engineering and Operational Research*, *2*(1), 13-23. https://doi.org/10.31181/smeor21202526
[6] Van, D. D., Chou, C. C., & Chang, K. C. (2023). Numerical and experimental study of two-vehicle overtaking process. *Advances in Mechanical Engineering*, *15*(12). https://doi.org/10.1177/16878132231221044
[7] Pasala, K., Bhargav, A., Jeevan Rao, H., Sreenath Reddy, K., & Seshaiah Naidu, T. V. (2014). A CFD Investigation into the flow distribution on a car passing by a truck. *International Journal of Current Engineering and Technology*, *2*(2), 525-528. https://doi.org/10.14741/ijcet/spl.2.2014.99
[8] Stojanovic, N., Grujic, I., & Boskovic, B. (2023). The influence of the crosswind on the lift coefficient, vehicle stability and safety. *Annals of Faculty Engineering Hunedoara - International Journal of Engineering*, *21*(4).
[9] Galamboš, S., Poznanović, N., Nikolić, N., Ružić, D. & Dorić, J. (2022). Experimental and Numerical Studies on Improvement of Aerodynamic Performance of a Semi-trailer Truck Model Using the Cabin Spoiler. *Tehnički vjesnik*, *29*(6), 1991-2000. https://doi.org/10.17559/TV-20211025173605
[10] Bonitz, S., Larsson, L., Lofdahl, L., & Broniewicz, A. (2015). Structures of Flow Separation on a Passenger Car. *SAE International Journal of Passenger Cars - Mechanical Systems*, *8*(1), 177-185. https://doi.org/10.4271/2015-01-1529
[11] She, R., Ouyang, Y., & Al-Qadi, I. L. (2018). *CDF Analysis and Prediction Model for Air Resistance on Platooned Freight Trucks*. (Report No. ICT-20-011). Illinois Center for Transportation. https://doi.org/10.36501/0197-9191/20-011
[12] Grm, A. & Batista, M. (2017). Vehicle Aerodynamic Stability Analysis under High Crosswinds. *Strojniški vestnik - Journal of Mechanical Engineering*, *63*(3), 191-200. https://doi.org/10.5545/sv-jme.2016.4095
[13] Menter, F. R., Lechner, R., & Matyushenko, A. (2021). *Best Practice: RANS Turbulence Modeling in Ansys CFD*.
[14] Alic, D., Matijošius, J., & Kilikevičius, A. (2025). Numerical Modelling of the Crosswind Influence On Vehicle Aerodynamics in Highway Traffic Conditions. *Facta Universitatis Series: Mechanical Engineering*, *23*(1), 65-77. https://doi.org/10.22190/FUME241212009A
[15] Bodhisagar, J. T. & Bajaj, P. S. (2022). A review on the effect of aerodynamics on car overtaking truck using CFD analysis method. *International Research Journal of Engineering and Technology*, *9*(8), 1273-1279.
[16] ANSYS. *Governing Equations of Fluid using Ansys Fluent*.
[17] Ma, X., Li, J., Zhao, J., & Chen, J. (2025). Aerodynamic characteristics of the race car in pitch and roll attitude. *International Journal of Numerical Methods for Heat & Fluid Flow*, *35*(1), 330-357. https://doi.org/10.1108/HFF-05-2024-0375
[18] Brandt, A., Jacobson, B., & Sebben, S. (2021). High speed driving stability of road vehicles under crosswinds: an aerodynamic and vehicle dynamic parametric sensitivity analysis. *International Journal of Vehicle System Dynamics*, *60*(7), 2334-2357. https://doi.org/10.1080/00423114.2021.1903516
[19] 3D Models. *Truck*.
[20] *BMW 1 Series Technical Data*.
[21] ANSYS. *Evaluation of Gradients and Derivatives*.
[22] ANSYS. *Pressure-Velocity Coupling*.
[23] Zhang, C., Bounds, C. P., Foster, L., & Uddin, M. (2019). Turbulence modeling effects on the CFD predictions of flow over a detailed full-scale sedan vehicle. *Fluids*, *4*(3), 148. https://doi.org/10.3390/fluids4030148
[24] Gu, Y., Liu, Y., Shen J., & Wang, D. (2023).Optimization of Reynolds number's effects on aerodynamic drag and automotive performance. *Theoretical and Natural Science*, *13*(1), 144-149. https://doi.org/10.54254/2753-8818/13/20240823
[25] Shao, N., Yao, G., Zhang, C., & Wang, M. (2017).A research into the flow and vortex structures around vehicles during overtaking maneuver with lift force included. *Advances in Mechanical Engineering*, *9*(9). https://doi.org/10.1177/1687814017732892
[26] Ghani, I. A., Hassan, R., Amin, I., Suhan, A., Husni, K., Didane, D. H., & Manshoor, B. (2023). Computational fluid dynamics (CFD) study on the aerodynamic of truck. *Journal of Design for Sustainable and Environment*, *5*(2), 23-27.
[27] Favre, T. (2011). *Aerodynamics simulations of ground vehicles in unsteady crosswind*. Doctoral Thesis, KTH School of Engineering Sciences, KTH Royal Institute of Technology.
[28] Van, D. D., Chou, C. C., & Chang, K. C. (2022). Aspects on numerical simulation of overtaking process between two vehicles. *Journal of Aeronautics, Astronautics and Aviation*, *54*(2), 161-178.
[29] Zhu, H. (2021). *Aerodynamic Analysis of Utility Truck Safety In Severe Environments*. Master's thesis, University of Alabama at Birmingham.

Contact information:

Daniela Delia ALIC, PhD Phys. M. Sc. Eng., Lecturer
(Corresponding author)
Politehnica University of Timisoara, Faculty of Engineering Hunedoara,
Revolutiei Street 2, 331128, Hunedoara, Romania
E-mail: daniela.alic@upt.ro

Luisa Izabel DUNGAN, PhD, Assoc. Professor
Politehnica University of Timisoara, Faculty of Mechanical Engineering,
Mihai Viteazu Street 1, 300222 Timisoara, Romania
E-mail: luisa.dungan@upt.ro

Milan RACKOV, PhD, Full Professor
University of Novi Sad, Faculty of Technical Sciences,
Trg Dositeja Obradovica 6, 21000 Novi Sad, Serbia
E-mail: racmil@uns.ac.rs

Marian GRECONICI, PhD, Full Professor
Politehnica University of Timisoara, Dep. Fundamental of Physics for Engineers,
Vasile Parvan Street 2, 300223 Timisoara, Romania
E-mail: marian.greconici@upt.ro

Carmen Inge ALIC, PhD, Assoc. Professor
Politehnica University of Timisoara, Faculty of Engineering Hunedoara,
Revolutiei Street 2, 331128, Hunedoara, Romania
E-mail: carmen.alic@upt.ro